

Silica-Alumina-Niobia ($\text{SiO}_2/\text{Al}_2\text{O}_3/\text{Nb}_2\text{O}_5$) Matrix Obtained by the Sol-gel Processing Method: New Material for Online Extraction of Zinc Ions

César Ricardo T. Tarley,^{*,a,b} Thiago C. de Ávila,^a Mariana G. Segatelli,^a
Giovana de F. Lima,^a Gabrielly dos S. Peregrino,^d Carla W. Scheeren,^c
Silvio Luís P. Dias^c and Emerson S. Ribeiro^d

^aDepartamento de Ciências Exatas, Universidade Federal de Alfenas, 37130-000 Alfenas-MG, Brazil

^bInstituto Nacional de Ciência e Tecnologia (INCT) de Bioanalítica, Universidade Estadual de Campinas, Cidade Universitária Zeferino Vaz s/n, 13083-970 Campinas-SP, Brazil

^cInstituto de Química, Universidade Federal do Rio Grande do Sul, 91501-970 Porto Alegre-RS, Brazil

^dInstituto de Química, Universidade Federal do Rio de Janeiro, 21941-909 Rio de Janeiro-RJ, Brazil

No presente trabalho foi avaliado um novo material como adsorvente, $\text{SiO}_2/\text{Al}_2\text{O}_3/\text{Nb}_2\text{O}_5$ (designado SiAlNb), empregado na determinação e pré-concentração *online* de Zn^{2+} por um método espectrofotométrico por injeção em fluxo. O método de pré-concentração é baseado na adsorção de Zn^{2+} em meio alcalino (pH 9,0) sobre a superfície de SiAlNb. A etapa de eluição é realizada usando solução de HNO_3 e é seguida da reação dos íons Zn^{2+} com 1-(2-piridilazo)-2-naftol (pan) na presença de Tween-80 em solução amoniacal (pH 9,3). O complexo formado, $[\text{Zn}(\text{pan})_2]$, é posteriormente determinado a 560 nm. O método apresentou faixa linear entre 7,6 e 180,0 $\mu\text{g L}^{-1}$ ($r = 0,9992$) e limites de detecção e quantificação de 2,3 e 7,6 $\mu\text{g L}^{-1}$, respectivamente. De acordo com o modelo linear de Langmuir, a capacidade máxima de adsorção foi de 7,0 mg de Zn^{2+} por grama de SiAlNb. O método proposto foi aplicado com sucesso na determinação de Zn^{2+} em amostras de água (lago, mineral e torneira) e material certificado de referência (TORT-2 Lobster Hepatopancreas).

In the present work, a new material, $\text{SiO}_2/\text{Al}_2\text{O}_3/\text{Nb}_2\text{O}_5$ (designated as SiAlNb), was evaluated as an adsorbent in a flow injection spectrophotometric method for online preconcentration and determination of trace amounts of Zn^{2+} ions. The preconcentration method is based on Zn^{2+} adsorption onto the surface of SiAlNb in alkaline medium (pH 9.0). The elution step is carried out using HNO_3 solution, followed by reaction of the Zn^{2+} ions with 1-(2-pyridylazo)-2-naphthol (pan) in ammoniacal buffer solution (pH 9.3) containing Tween-80. The $[\text{Zn}(\text{pan})_2]$ complex formed is determined at 560 nm. The method presented a linear range between 7.6 and 180.0 $\mu\text{g L}^{-1}$ ($r = 0.9992$) and limits of detection and quantification of 2.3 and 7.6 $\mu\text{g L}^{-1}$, respectively. According to the Langmuir linear model, the maximum adsorption capacity was found to be 7.0 mg of Zn^{2+} g⁻¹ of SiAlNb. The proposed method was successfully applied to the Zn^{2+} determination in water samples (lake, mineral, tap) and certified reference material (TORT-2 Lobster Hepatopancreas).

Keywords: adsorbent preconcentration system, zinc ions, silica-alumina-niobia, sol-gel process

Introduction

Current research in the field of analytical sciences has basically been focused on the enhancement of technique performance, such as in miniaturization, automation capabilities and enhanced power detection, as well as on sample preparation, aiming at solving instrumental

problems.¹ Undoubtedly, solid phase extraction (SPE) is considered one of the most representative techniques for sample preparation, enabling both the removal of severe matrix interferences and the achievement of accentuated enrichment factors. Moreover, other advantages can be pointed out, such as easy automation with flow injection systems, easy recovery of solid phase and, in many cases, no requirement for the use of toxic solvents.^{2,3} These features enable SPE to be widely used in combination

*e-mail: ctarleyquim@yahoo.com.br

with relatively simple detection techniques as well as sophisticated equipments. Literature presents a great number of adsorbents which are traditionally classified as inorganic-based ones, mainly Al_2O_3 and SiO_2 ; organic-based ones, including natural adsorbents; organic polymers (chelating resins or non-polar polymers); hybrid organic-inorganic polymers and carbonaceous adsorbents (activated carbon, fullerene and carbon nanotubes).^{4,5} Bearing in mind the application of SPE for metal ions, depending upon the choice of materials (mainly those organic polymers with medium polarity), it is necessary to use chelating agents for metal ions so that selectivity can be achieved. Other adsorbents, such as the natural ones, do not usually present selectivity and chemical stability. Therefore, there have been attempts to develop materials with novel and interesting properties through variation of their chemical composition and physical dimensions. New solid adsorbents should possess an excellent specific surface area, highly stable chemical structure over a wide pH range, high adsorption capacity, excellent swelling resistance in different solvents at high pressure, fast and quantitative adsorption and elution, high mass exchange and easy and low cost synthesis. These features are somewhat observed in silica (SiO_2), but the silica matrix used to adsorb metal ions in aqueous solution presents some limitations associated to low selectivity, since the silanol groups (Si-OH) are weakly acidic, and reduced chemical stability in alkaline medium due to hydrolysis of siloxane groups, which is favoured at high pH values.⁶ Thus, close attention has been widely paid for searching organically and inorganically modified silica. This later approach has been based on preparation of $\text{SiO}_2/\text{M}_x\text{O}_y$ binary oxides obtained by the sol-gel processing method, in which the mechanical properties of the silica matrix are combined with the chemical properties of bulk of the metal oxides (M_xO_y).

The sol-gel process also permits to obtain a solid with controlled porosity, and the metal oxide can be obtained as highly dispersed particles in the matrices.⁷ Basically, the procedure consists in the reaction between tetraethylorthosilicate, $\text{Si}(\text{OEt})_4$, and the metal oxide precursor, $\text{M}(\text{OR}')_y$, showed in equation 1:



The product, $\text{SiO}_2/\text{M}_x\text{O}_y$, has found many applications in recent years.⁸⁻²² One of the greatest interests is its use as a porous substrate to immobilize electroactive species and the possibility to prepare a series of electrochemical sensors (chemically modified electrodes).^{8-11, 23-26} The metal oxides dispersed in the silica matrix are usually

refractory, including TiO_2 , Al_2O_3 , Sb_2O_5 and Nb_2O_5 . They present acid and basic properties and therefore can be used for adsorbing metal ions and anionic species depending upon the pH range.²⁷ It is also important to emphasize that the metal oxide dispersed on the silica matrix presents chemical and physical properties different from those observed for bulk metal oxide, including a higher capacity for ion exchange.²⁸

The use of $\text{SiO}_2/\text{M}_x\text{O}_y$ binary oxides in analytical approaches has been reported for silica-niobia ($\text{SiO}_2/\text{Nb}_2\text{O}_5$),²⁹ silica-titania ($\text{SiO}_2/\text{TiO}_2$),³⁰ silica-zirconium(IV)-phosphate ($\text{SiO}_2/\text{Zr}(\text{H}_2\text{PO}_4)_2$),³¹ and silica-zirconia ($\text{SiO}_2/\text{ZrO}_2$)³², where they were successfully used for extraction/preconcentration of trace metals. Nevertheless, to the best of our knowledge, the oxide mixture dispersed on the silica matrix, *i.e.*, $\text{SiO}_2/\text{M}_x\text{O}_y/\text{N}_z\text{O}_w$, has not been investigated for analytical purposes concerning metal preconcentration. Therefore, as Al_2O_3 and Nb_2O_5 present Brønsted acid and base properties, besides being used as catalysts³³ and ion exchangers,³⁴ we highlight, in the present work, the use of this oxide mixture dispersed onto silica matrix (SiAlNb) as a new adsorbent for metal ions for the first time. The Al_2O_3 and Nb_2O_5 oxides are chemically stable in a wide pH range, and Nb_2O_5 , in particular, is soluble only in HF and hot H_2SO_4 .³⁵ Thus, the presence of these oxides on the silica matrix (mainly at high Nb_2O_5 concentration) makes the SiAlNb material chemically stable at high pH values.

Particular interest was given to zinc ions owing to their intrinsic importance in various biological systems, where it is found in more than 80 enzymes (as in carboxypeptidase, carbonic anhydrase, bovine superoxide dismutase, etc.)³⁶ and environmental samples, as well as to their trace amount commonly found in these samples. For example, the active site of the alcohol dehydrogenase (ADH) consists of a zinc atom, and ADH catalyzes the transfer of a hydride ion from NADH to acetaldehyde, forming ethanol.³⁷ Zinc deficiency can produce hair loss, diarrhea, impotence and sexual immaturity, apathy, chronic liver disease, chronic renal disease, amnesia, fatigue, and other chronic illnesses.³⁸ Also, zinc compounds such as zinc chloride, sulfide and oxide are widely employed in the industry. Thus, there is great interest in determining the presence of zinc in various types of samples, such as environmental, biological, industrial, etc. The feasibility of the new SiAlNb adsorbent for zinc ions was investigated by the development of an adsorbent flow preconcentration system coupled to UV-Vis spectrophotometry. The proposed method shows attractive features as a new and efficient system for zinc determination in trace levels in water and biological samples.

Experimental

Apparatus

A Femto UV-Vis spectrophotometer (São Paulo, Brazil), model 482, equipped with a flow cell of 1 cm optical length, was used for FIA measurements. Data acquisition was carried out from an interfaced (Advantech) PCL 711S mode and a computational program was developed in an EXCEL® spreadsheet, using macros of Visual Basic®. An Ismatec Model IPC peristaltic pump (Ismatec IPC-08, Glattbrugg, Switzerland) furnished with Tygon® tubes was used to propel all sample and reagent solutions. The preconcentration/elution steps were selected by using a home-made injector commutator made of Teflon® (PTFE, polytetrafluoroethylene). Adjustment of sample pH was done by using a Handylab 1 Schott pHmeter (Stafford, UK). A Shimadzu AA-6800 flame atomic absorption spectrometer (FAAS) (Shimadzu, Tokyo, Japan) was also used in this study. The specific surface area of the solid, previously degassed at 250 °C under vacuum, was determined by the BET (Brunauer, Emmett and Teller) multipoint technique on an ASAP 2010 Micromeritics apparatus, using nitrogen as a probe. The Al_2O_3 and Nb_2O_5 contents in the SiAlNb sample were determined by using energy dispersive X-ray fluorescence analysis (EDFRX) on a model EDX 800 HS from Shimadzu. For the scanning electron microscopy (SEM) and electron dispersive spectroscopy (EDS) analyses, the sample was dispersed on double face conductive tape on a copper support and coated with gold before the experiment. Sample was observed by using a JEOL model JSM 5800 scanning electron microscope, with 20 kV and 330 times of magnification.

The infrared spectra were obtained as KBr pellets (1 wt.%) on a NICOLET Magna-IR 760 spectrophotometer with 4 cm^{-1} resolution and 16 cumulative scans.

Reagents and solutions

The solutions were prepared with water obtained from a Milli-Q purification system (Millipore, Bedford, MA, USA) to a resistivity of 18.2 $\text{M}\Omega\text{ cm}$, and analytical grade chemical reagents. In order to prevent metal contamination, the laboratory glassware was kept overnight in a 10% (v/v) HNO_3 solution. Zinc standard solutions were prepared daily by appropriate dilution of a 1000 mg L^{-1} zinc solution (Merck, Darmstadt, Germany).

Ammoniacal, acetate, borate and phosphate buffer solutions were prepared from their respective sodium salts purchased from Merck, without further purification.

Concentrated HNO_3 and 30% (v/v) H_2O_2 (Merck) were used for the decomposition of the certified reference material in microwave oven (Milestone, Sorisole, Italy). HNO_3 was previously purified from a sub-boiling system (Milestone).

The chelating agent 1-(2-piridylazo)-2-naphtol (pan) and the surfactant Tween-80 were acquired from Vetec (Rio de Janeiro, Brazil). For the preparation of SiAlNb, tetraethylorthosilicate at 98%, aluminum isopropoxide at 98%, niobium(V) chloride at 99% and trifluoroacetic acid, all from Aldrich (St. Louis, USA), were used.

Preparation of SiAlNb mixed oxide

The new material $\text{SiO}_2/\text{Al}_2\text{O}_3/\text{Nb}_2\text{O}_5$, designated as SiAlNb, was prepared according to the following procedure: Into 100.0 mL of a 50% (v/v) solution of ethanol/TEOS (TEOS = tetraethylorthosilicate), 5.6 mL of 3.5 mol L^{-1} HCl were added. The mixture was stirred for 3 h at 60 °C. After the pre-hydrolysis step, 4.4 g of aluminum isopropoxide (dissolved in small amounts of trifluoroacetic acid) and 6.7 g of NbCl_5 (previously solubilized in ethanol under a nitrogen atmosphere) were added and the resulting mixture was stirred for 2 h at 60 °C. The mixture was stirred for another period of 12 h at room temperature. The solvent was slowly evaporated at 60 °C until gel formation. The gel so obtained was ground ($\leq 250\ \mu\text{m}$) and the resulting particles were washed with ethanol in a soxhlet extractor for 4 h. Finally, the material was washed with 100 mL of 0.1 mol L^{-1} HNO_3 , deionized water and ethanol, followed by drying under vacuum (1.3×10^{-2} Pa) for 2 h at room temperature and then stored.

Adsorbent flow preconcentration system

The diagram of the flow preconcentration system is displayed in Figure 1. At the preconcentration step position (Figure 1a), 20.0 mL of the sample buffered at pH 9.0 were percolated through a minicolumn of SiAlNb (150 mg) at 4.0 mL min^{-1} flow rate. After this stage, by switching the central part of the injector commutator, a stream of 0.50 mol L^{-1} HNO_3 displaces the zinc ions at 1.0 mL min^{-1} flow rate. Afterwards, the eluted zinc ions react with 100.0 $\mu\text{mol L}^{-1}$ pan solution (pH 9.3) at 2.0 mL min^{-1} flow rate. The $[\text{Zn}(\text{pan})_2]$ complex is pumped into the spectrophotometer, where the absorbance measurements are continuously made at 560 nm. All absorbance signals were taken as peak height. The chelating pan was adopted in this work because it is a reagent broadly applicable to heavy metals and very common in laboratory.

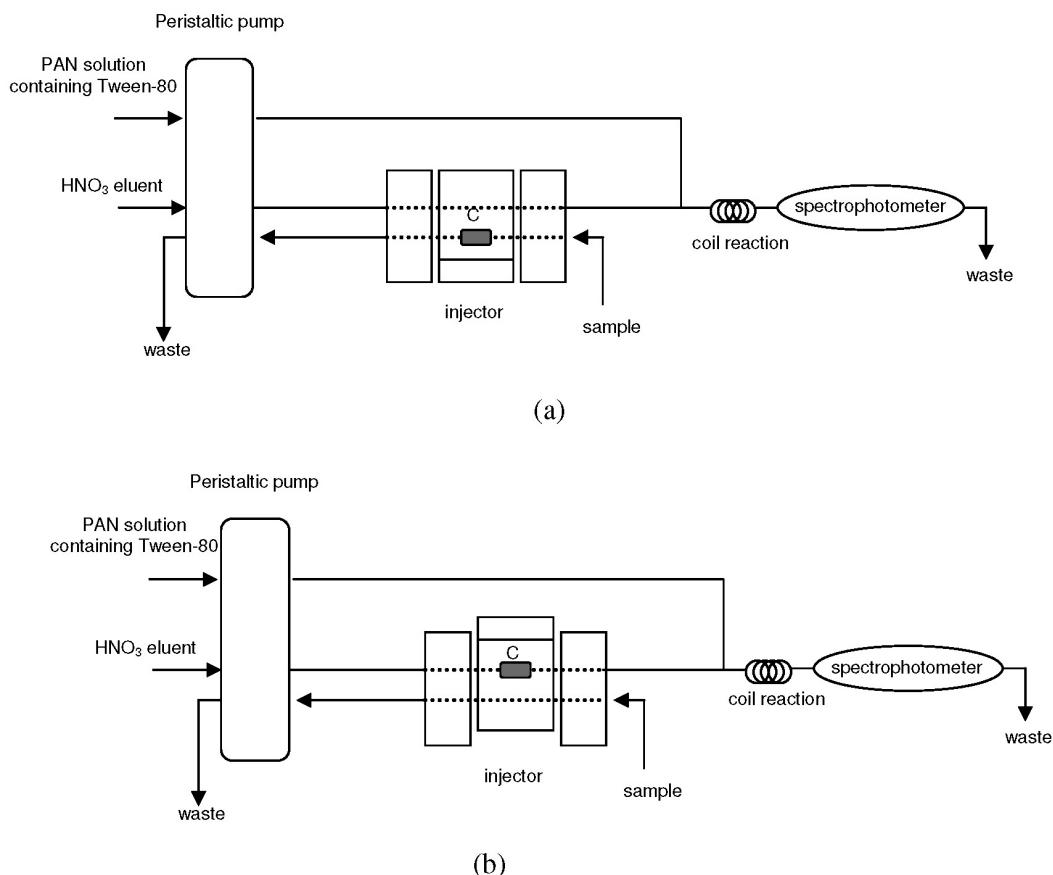


Figure 1. Schematic diagram of the adsorbent flow preconcentration system of zinc ions onto SiAlNb with spectrophotometric determination. (a) Preconcentration stage and (b) elution stage. C = minicolumn packed with SiAlNb. For more details, see text.

Adsorption isotherm

The zinc adsorption experiments onto SiAlNb were carried out at 298 K using the batch technique. 20.0 mL of zinc solution, with concentrations increasing from 0.1 up to 10 mg L⁻¹, were shaken during 10 min in 0.05 mol L⁻¹ ammoniacal buffer (pH 9.0). At the end of this equilibrium time, the zinc adsorption by SiAlNb was determined by measuring the initial and final concentration of zinc by FAAS. In order to determine the maximum adsorption capacity (MAC), all batch experimental data were fitted to the linear Langmuir and Freundlich isotherm models.³⁹

Sample preparation

The devised method was applied for zinc determination in lake water, mineral water and tap water. Mineral and tap water samples were acquired from local supermarkets and from UNIFAL-MG campus and analyzed immediately after pH adjusting with buffer solution. Lake water samples were collected in polypropylene flasks from a lake near Alfnas city and immediately acidified with HNO₃ solution until a pH sample of 2.0 was attained. Afterwards, the samples

were filtered through 0.45 μm cellulose acetate membranes under vacuum and the pH was adjusted with buffer solution. Besides these samples, the feasibility of the methodology was also evaluated by analysis of certified reference material (TORT-2 Lobster Hepatopancreas). About 100 mg of the sample were placed into Teflon® flasks, followed by addition of 10 mL concentrated HNO₃ and 4 mL 30% (v/v) H₂O₂. The heating program of the microwave oven was then employed in two steps. A 400 W power was applied during 5 min, with further increase to 700 W, which was maintained during 10 min. After this step, 4 mL 30% (v/v) H₂O₂ were added to the sample, which was heated on a hot plate to near dryness, then cooled to room temperature and dissolved in ammoniacal buffer solution. Any contamination source was checked by using blank solutions.

Results and Discussion

Characterization of SiAlNb

The sample presented characteristics of a porous material and a remarkable surface area around 309 m² g⁻¹ obtained by the BET (Brunauer, Emmet, Teller) method.

In addition, it revealed mesopores, which contribute to a higher surface area and allow Zn^{2+} ions diffusion into the pores. These features are highly desirable for the proposed application of this solid adsorbent in flow preconcentration system for metal determination.

The results obtained for the Al_2O_3 and Nb_2O_5 amounts incorporated in the material SiAlNb, obtained by EDFRX, were 2.1 wt.% and 33.6 wt.%, respectively. The value of the 2.1 wt.% for the Al_2O_3 was somewhat lower than expected, probably owing to the pH of the reaction medium, which was not favorable to the complete hydrolysis of aluminum isopropoxide. However, the material SiAlNb is an excellent ion exchanger.

A typical SEM micrograph of the SiAlNb material is shown in Figure 2. The image indicates that the particles of Al_2O_3 and Nb_2O_5 are dispersed on the SiO_2 surface within the magnification used. A few white agglomerated particles are due to Al_2O_3 and Nb_2O_5 and can be detected on the surface as isolated islands in Figure 2A. At the studied level, the material seems homogeneous, as can be

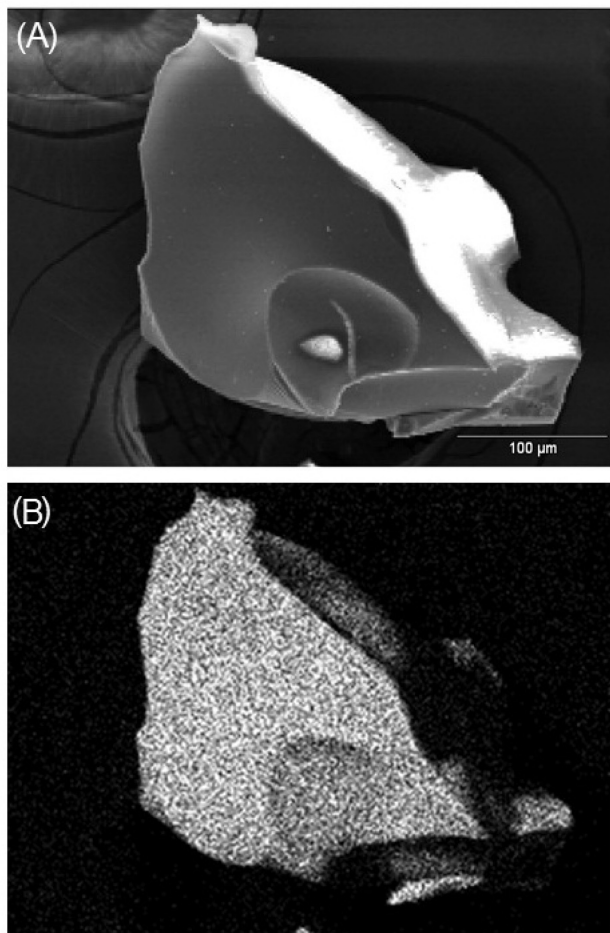


Figure 2. (A) Scanning electron microscopy image of SiAlNb and (B) the corresponding energy dispersive scanning image (EDS) of aluminium and niobium. Conditions: accelerating voltage of 20.0 kV and magnification of 330 (scale bar 100 μm).

seen in Figure 2B (the energy dispersive scanning image, EDS). The Figure 2B showed that the Al and Nb atoms are dispersed without any detectable phase segregation of the oxide particles in the matrix and are present on the SiAlNb surface under the magnification used. A good dispersion of the metal oxides in the matrix is an important feature for the application of the material as a new adsorbent for trace metals using flow injection spectrophotometry.

Figure 3 shows the infrared spectra of SiO_2 (---) and SiAlNb (—) obtained by the sol-gel process. The two spectra are very similar, although the bands recorded for SiAlNb are somewhat broader and some of them shift toward lower frequencies. This behavior is consistent with the infrared spectra obtained by Aronne *et al.*⁴⁰ for Nb_2O_5 - SiO_2 obtained by the sol-gel process with different concentrations of Nb_2O_5 [between $(\text{Nb}_2\text{O}_5)_{0.025}(\text{SiO}_2)_{0.975}$ and $(\text{Nb}_2\text{O}_5)_{0.2}(\text{SiO}_2)_{0.8}$], suggesting that the bands are progressively influenced by the amount of Nb_2O_5 . The infrared spectra indicate that the SiO_2 network is only slightly disturbed by the presence of the metal oxides, suggesting that Al_2O_3 and Nb_2O_5 are dispersed on the matrix, as observed from EDS data.

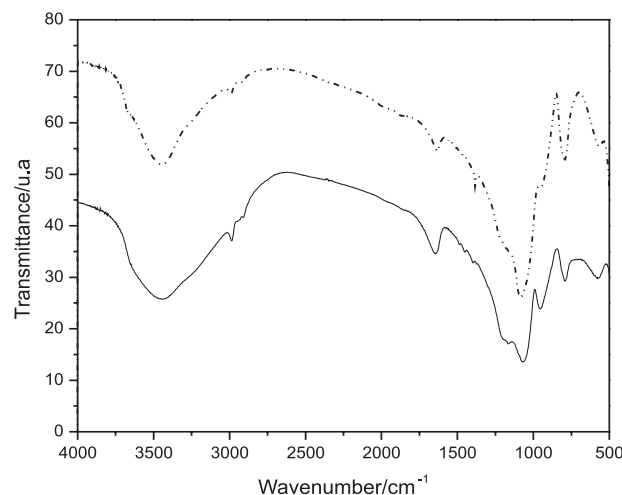


Figure 3. Infrared spectra of materials obtained by the sol-gel process: (---) SiO_2 and (—) SiAlNb.

Optimization of Adsorbent Preconcentration System

The influence of sample pH on the adsorption of zinc ions onto SiAlNb was studied from pH 4.0 to 10.0. For this study, the zinc standard solutions were buffered with different types of buffers, whose concentrations were maintained at 0.05 mol L⁻¹. Acetate for pH 4.0 and 5.0, phosphate for pH 6.0 up to 8.0 and borate for pH 9.0 and 10.0 were used. The oxides grafted on silica surface present Brønsted acid and base properties. Therefore, the retention of Zn^{2+} ions takes place by electrostatic interaction with oxygen atoms bonded to metal

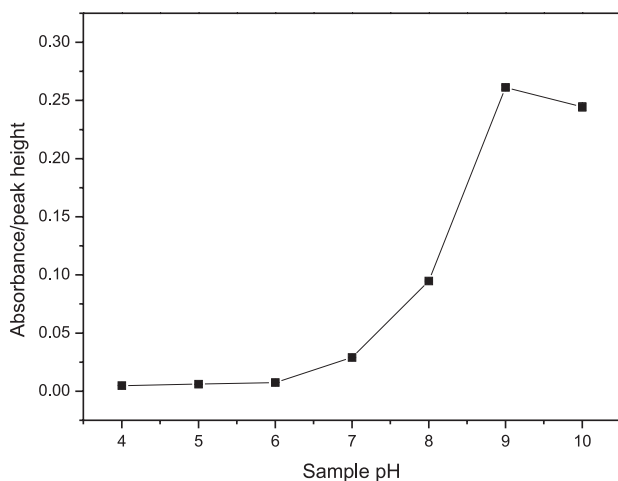


Figure 4. Effect of sample pH on the adsorption of $100 \mu\text{g L}^{-1}$ of Zn^{2+} onto 100 mg SiAlNb . Elution with $0.1 \text{ mol L}^{-1} \text{HNO}_3$; sample flow rate: 5.0 mL min^{-1} ; eluent flow rate: 1.0 mL min^{-1} ; sample buffer: 0.1 mol L^{-1} ; [pan]: $100 \mu\text{mol L}^{-1}$; length of reaction coil: 1 m . The errors were less than 1.5% .

(Si-O-Al-O-H and Si-O-Nb-O-H).^{41,42} As a consequence, the adsorption is very low at low pH values owing to the protonation of the oxygen centers. On the other hand, higher adsorption of Zn^{2+} is observed in alkaline medium. As can be seen in Figure 4, an increase in the analytical signal was observed by increasing the sample pH. Moreover, the electrostatic retention of CH_3COO^- or H_2PO_4^- anions onto the positively charged surface material also contributes to the reduced adsorption rate of Zn^{2+} ions. At pH values above 7.0, the adsorption increases significantly because the SiAlNb acquires negative charge and, as a consequence, an effective retention of Zn^{2+} ions occurs. It must be emphasized that, within the pH range from 8.0 and 9.0, the presence of PO_4^{3-} and BO_3^{3-} can lead to the precipitation of Zn^{2+} ions or their complexation, respectively, and it would imply a decrease in adsorption rate. However, the very high analytical signal observed even in alkaline medium confirms that adsorption takes place, in fact, by retention of Zn^{2+} ions onto the negatively charged adsorbent surface. Above pH 9.0, the adsorption was less effective, probably due to the formation of $[\text{Zn}(\text{OH})_4]^{2-}$, which is not retained by the adsorbent. Thus, the sample pH of 9.0 was chosen for further experiments. As previously mentioned, the presence of Al_2O_3 and Nb_2O_5 (especially the high concentration of Nb_2O_5 in our case) makes the silica matrix stable at pH 9.0, and the hydrolysis of siloxane groups is not observed due to the high chemical stability of the material SiAlNb.

The effect of the sample flow rate was examined in the 2.0 – 8.0 mL min^{-1} range. As shown in Figure 5, by employing a low preconcentration flow rate ranging from 2.0 up to 4.0 mL min^{-1} , differences in the analytical signal were observed. However, when the work was carried out with a preconcentration flow rate higher than 4.0 mL min^{-1}

the analytical signal was unsatisfactory, indicating that the kinetic of mass transfer of Zn^{2+} towards the adsorbent sites is not so fast and depends on the flow rate. Therefore, the preconcentration flow rate of 4.0 mL min^{-1} was chosen for this study.

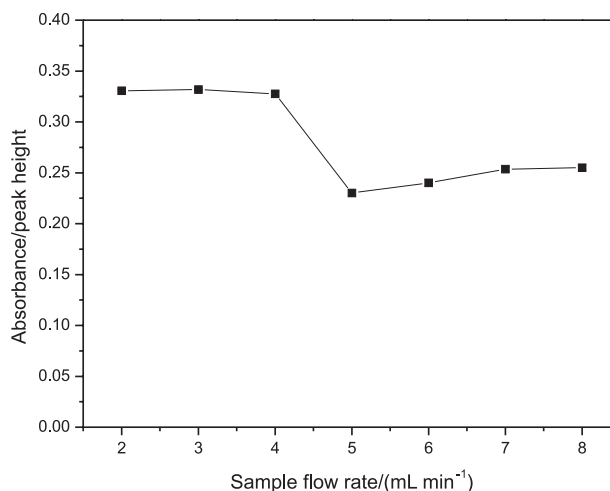


Figure 5. Effect of sample flow rate on the adsorption of $100 \mu\text{g L}^{-1}$ of Zn^{2+} onto 100 mg de SiAlNb . Sample pH: 9.0; elution with $0.1 \text{ mol L}^{-1} \text{HNO}_3$; eluent flow rate: 1.0 mL min^{-1} ; [pan]: $100 \mu\text{mol L}^{-1}$; length of reaction coil: 1 m . The errors were less than 1.5% .

In order to assess the effect of the type of buffer on the adsorption of zinc ions onto SiAlNb, the preconcentration step was carried out by buffering the sample with ammoniacal or borate buffers at 0.05 mol L^{-1} . An increase of *ca.* 30% in the analytical signal was observed when ammoniacal buffer was used instead of borate buffer. This result can possibly be explained by a higher zinc borate complex formation at pH 9.0 than ammoniacal complex formation.⁴³ Therefore, ammoniacal buffer was selected for further experiments.

The effect of buffer concentration was studied by ranging ammoniacal buffer from 0.001 up to 0.2 mol L^{-1} . Figure 6 illustrates the effect of increasing concentrations of buffer solution on the retention of Zn^{2+} ions onto SiAlNb and, as can be seen, the increase of the buffer concentration up to 0.05 mol L^{-1} increases the analytical signal. A lower buffer concentration could not be used because it would not be feasible to maintain the sample buffered when the nitric acid solution is employed as eluent. The analytical signal decreases significantly as the buffer concentration exceeds 0.05 mol L^{-1} . These results suggest that the formation of $[\text{Zn}(\text{NH}_3)_4]^{2+}$ may influence the adsorption rate of Zn^{2+} ions onto SiAlNb. Thus, a buffer concentration of 0.05 mol L^{-1} was selected as the best condition.

The concentration of pan plays an important role in the analytical signal. Its concentration must be sufficiently high to guarantee the total complexation of zinc. The studied range was from 100.0 to $800.0 \mu\text{mol L}^{-1}$ (Figure 7). For all

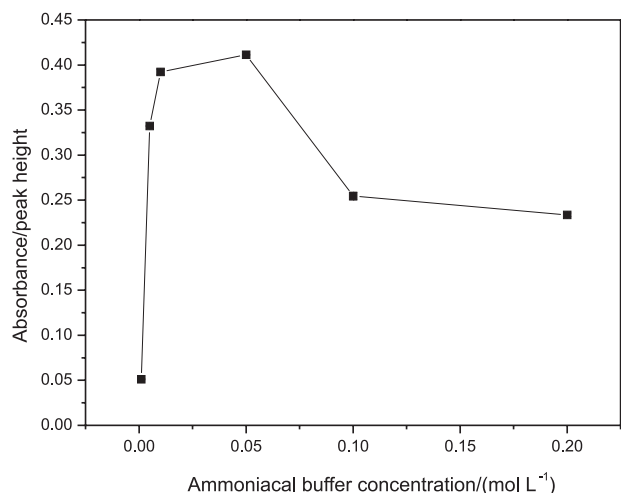


Figure 6. Effect of sample buffer concentration on the adsorption of $100 \mu\text{g L}^{-1}$ of Zn^{2+} onto 100 mg de SiAlNb. Sample pH: 9.0; sample flow rate: 4.0 mL min^{-1} ; elution with $0.1 \text{ mol L}^{-1} \text{ HNO}_3$; eluent flow rate: 1.0 mL min^{-1} ; [pan]: $100 \mu\text{mol L}^{-1}$; length of reaction coil: 1 m . The errors were less than 1.5%.

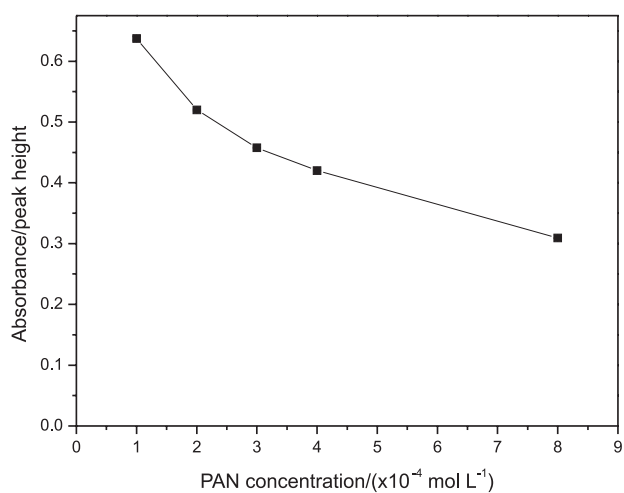


Figure 7. Effect of pan concentration on the complexation of Zn^{2+} . Sample pH: 9.0; sample flow rate: 4.0 mL min^{-1} ; elution with $0.1 \text{ mol L}^{-1} \text{ HNO}_3$; eluent flow rate: 1.0 mL min^{-1} ; length of reaction coil: 1 m ; sample buffer concentration of 0.05 mol L^{-1} . The errors were less than 1.5%.

studied values, there is an excess of pan as compared to zinc ions. However, the excessive concentration of chelating agent in the medium can reduce the molar absorptivity of the $[\text{Zn}(\text{pan})_2]$ complex. Thus, the concentration of $100.0 \mu\text{mol L}^{-1}$ pan was adopted for further experiments.

The effect of the length of the reaction coil was examined over the range $0.5\text{--}4.0 \text{ m}$ (Figure 8). As observed, the analytical signal increased with increasing coil length, so that the Zn^{2+} ions and pan can react completely. By using a coil length higher than 3.0 m , a high degree of dispersion is observed and, as a consequence, the peak height decreases. Therefore, a length of reaction coil of 2.0 m was chosen as the optimal parameter, as a compromise between sensitivity and time of analysis.

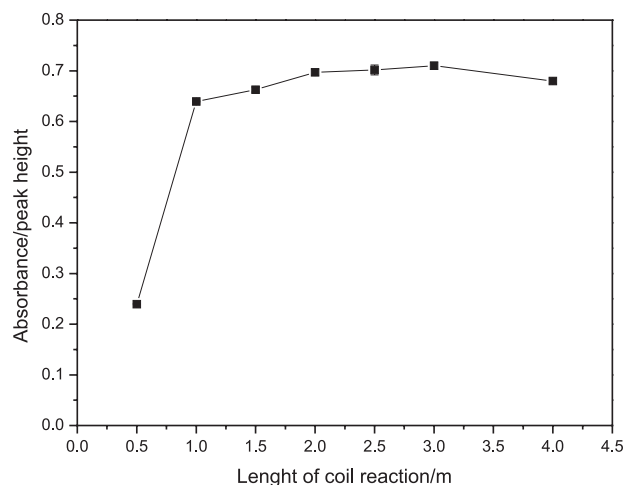


Figure 8. Effect of length of reaction coil on the complexation of Zn^{2+} with pan. Sample pH: 9.0; sample flow rate: 4.0 mL min^{-1} ; elution with $0.1 \text{ mol L}^{-1} \text{ HNO}_3$; eluent flow rate: 1.0 mL min^{-1} ; sample buffer concentration: 0.05 mol L^{-1} ; [pan]: $100 \mu\text{mol L}^{-1}$. The errors were less than 1.5%.

The effect of eluent concentration on complete desorption of Zn^{2+} from SiAlNb was studied using nitric acid solutions at different concentrations ($0.05\text{--}0.5 \text{ mol L}^{-1}$). As shown in Figure 9, for concentrations lower than 0.2 mol L^{-1} , a dramatic decrease in the analytical signal is observed, associated with memory effect after each preconcentration/elution step. Under these conditions, the eluent is not able to disrupt sufficiently the interaction of Zn^{2+} with the SiAlNb surface and subsequently release the metal ion. Quantitative elution is obtained by using concentrations higher than $0.2 \text{ mol L}^{-1} \text{ HNO}_3$. Nevertheless, above this concentration, the buffering capacity of the ammoniacal buffer is seriously diminished. So, $0.2 \text{ mol L}^{-1} \text{ HNO}_3$ as desorption agent was used in the system.

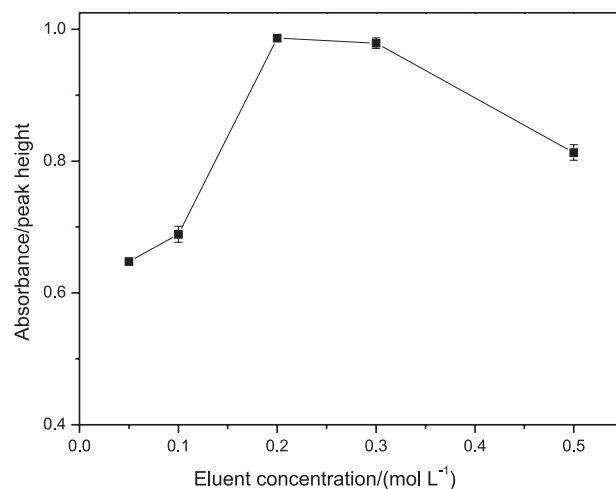


Figure 9. Effect of HNO_3 concentration on the Zn^{2+} desorption from 100 mg of SiAlNb. Sample pH: 9.0; sample flow rate: 4.0 mL min^{-1} ; eluent flow rate: 1.0 mL min^{-1} ; sample buffer concentration: 0.05 mol L^{-1} ; [pan]: $100 \mu\text{mol L}^{-1}$; length of reaction coil: 2 m .

Effect of foreign ions on preconcentration method

In order to investigate the selective separation and determination of zinc ions from real samples containing different metal ions, a 100 $\mu\text{g L}^{-1}$ zinc solution and increasing amounts of possible interfering ions were taken and submitted to the preconcentration procedure. The ratios analyte:concomitant employed were 1:1, 1:10 and 1:100 (m/v) for all metals evaluated. The results were compared with zinc preconcentration in the absence of concomitant. When the analytical signal was changed positively or negatively above 10%, the presence of interference in the procedure was considered. The maximum limit of each concomitant metal ion that did not interfere with zinc concentration was: Ni^{2+} (100 $\mu\text{g L}^{-1}$), Cd^{2+} (1000 $\mu\text{g L}^{-1}$), Co^{2+} (100 $\mu\text{g L}^{-1}$), Ca^{2+} (100 mg L^{-1}), Sb^{3+} (1000 $\mu\text{g L}^{-1}$), Hg^{2+} (100 mg L^{-1}), Pb^{2+} (1000 $\mu\text{g L}^{-1}$) and Mn^{2+} (100 $\mu\text{g L}^{-1}$). The absence of interference when using an analyte:concomitant ratio of 1:1 (m/v) is probably attributed to Pearson's definition of acids and bases.⁴⁴ Co^{2+} , Ni^{2+} , Mn^{2+} and Zn^{2+} are considered borderline cations and possess affinity for both hard ligands containing oxygen (O) and soft ligands containing sulfur (S). However, as Zn^{2+} is more polarizable and bigger than Co^{2+} , Ni^{2+} and Mn^{2+} ions, it is considered a very soft acid. Thus, as the oxygen atom bonded to the metal in Si-O-Al-O and Si-O-Nb-O becomes more polarizable, and as consequence a very soft base, explains fairly the preference of Zn^{2+} in detriment of Co^{2+} , Ni^{2+} and Mn^{2+} towards those oxygen atoms of SiAlNb. It can be inferred, from these results, that the method presents reasonable selectivity, once the amounts of these metals are lower in drinking and lake waters. This means that Zn^{2+} can be determined by UV-Vis spectrophotometry even in the presence of these metals, as will be demonstrated from the application of the method in real samples.

Adsorption isotherm

In order to determine the equilibrium time for transfer of Zn^{2+} ions between the solid and liquid phases, extractions in batch experiments for a series of solutions in a medium containing 0.05 mol L^{-1} ammoniacal buffer (pH 9.0) and 2.0 mg L^{-1} Zn^{2+} ions were carried out, according to the conditions optimized in the adsorbent flow preconcentration system. Results showed that the equilibrium time, ranging from 1 to 25 min, is attained in 10 min (data not shown). Thus, the mixtures have been shaken for 10 min to reach the equilibrium in the subsequent adsorption isotherm experiments.

Figure 10 shows the adsorption isotherm of Zn^{2+} ions onto SiAlNb, where a plateau was achieved when the

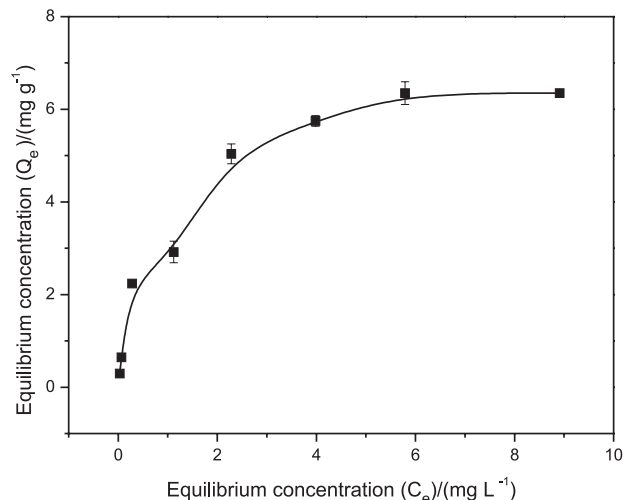


Figure 10. Adsorption isotherm of Zn^{2+} onto SiAlNb. For more details, see text.

equilibrium concentration in the mixture was 6.0 mg L^{-1} . The maximum amount of Zn^{2+} adsorbed per unit of surface area of SiAlNb, *i.e.*, the maximum adsorption capacity, was determined by employing the following linear Langmuir or Freundlich isotherm models.

The Langmuir linear model is given by: $C_e/Q_e = C_e/M + 1/(KM)$, where Q_e is the adsorbed amount of Zn^{2+} (mg g^{-1}), C_e the Zn^{2+} equilibrium concentration (mg L^{-1}) and M and K are, respectively, the maximum zinc adsorption capacity and the binding constant. This model establishes that adsorption takes place at a monolayer of adsorbent.

The Freundlich linear model is given by: $\log(Q_e) = \log(K_F) + \beta \log(C_e)$, where Q_e is the adsorbed amount of Zn^{2+} (mg g^{-1}), C_e the Zn^{2+} equilibrium concentration (mg L^{-1}), β is a constant and K_F is the Freundlich adsorption isotherm. This model establishes that adsorption is not restricted to the formation of a monolayer. According to Figure 11, the best correlation coefficient indicates that the experimental data fit very well the Langmuir linear model ($r = 0.99465$). Thus, the Langmuir model is the most favorable one and this result is somewhat expected, taking into consideration that, according to SEM and EDS data, the Al_2O_3 and Nb_2O_5 particles are dispersed onto silica matrix surface as isolated islands.

From the Langmuir linear model, the MAC, determined from the inverse of the angular coefficient, was 7.0 mg g^{-1} . This result shows that the adsorption capacity of SiAlNb towards Zn^{2+} ions is higher than that reported for other adsorbent materials such as amberlite XAD-2000 (4.80 mg g^{-1}),⁴⁵ zinc(II) ion-imprinted polymer (3.90 mg g^{-1}),⁴⁶ amberlite XAD-2 resin-pyrocatechol (1.85 mg g^{-1}),⁴⁷ silica gel-silicylaldoxime (2.61 mg g^{-1})⁴⁸ and amberlite XAD-2 resin-*o*-aminophenol (2.94 mg g^{-1}).⁴⁹

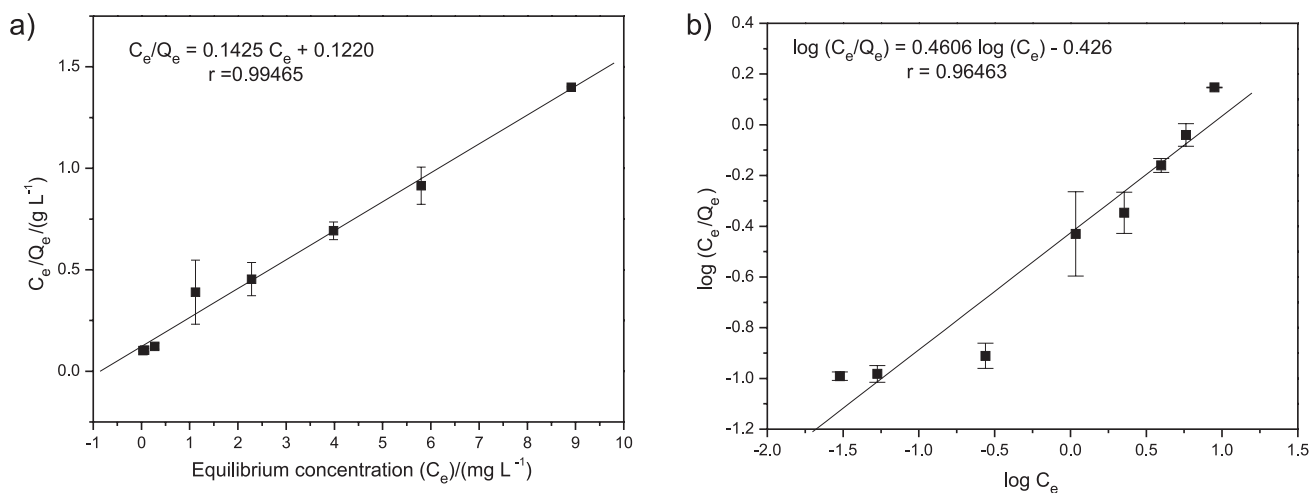


Figure 11. Linearization of adsorption isotherm using Langmuir and Freundlich models. For more details, see text

Characteristics of the adsorbent preconcentration flow system

The calibration graph (run for triplicate measurements at each point) for preconcentrating 20.0 mL of sample gave a linear range from 30.0 to at least 180.0 $\mu\text{g L}^{-1}$ ($r = 0.99926$), whose linear equation was $\text{Abs} = 3.45 \times 10^{-2} + 6.68 \times 10^{-3} [\text{Zn}^{2+}, \mu\text{g L}^{-1}]$. The precision of the method, expressed as the R.S.D., for the determination of 20.0 and 170.0 $\mu\text{g L}^{-1}$ Zn^{2+} , were 3.25 and 1.71%, respectively ($n = 10$). The linear equation obtained without the preconcentration system was $\text{Abs} = 3.64 \times 10^{-2} + 1.27 \times 10^{-4} [\text{Zn}^{2+}, \mu\text{g L}^{-1}]$. Therefore, the enrichment factor (EF), defined⁵⁰ as the ratio of the slopes of the linear equation of the calibration graphs before and

after the preconcentration, was 52.6. The concentration efficiency (CE) defines the preconcentration factor attained by an adsorbent flow preconcentration system during 1 min of preconcentration. Thus, as the entire time of preconcentration step was 5 min, the calculated CE was found to be 10.5 min^{-1} . The consumptive index (CI), defined as the volume of sample in milliliters consumed to achieve a unit EF, was 0.38 mL. The limits of detection and quantification, defined, respectively, as the concentration of analyte leading to a signal equivalent to three and ten times the S.D. of the blank signal plus the net blank intensity,⁵¹ were measured as 2.3 and 7.6 $\mu\text{g L}^{-1}$. The performance of the present adsorbent flow preconcentration method was compared with other methods for zinc preconcentration

Table 1. Features of different preconcentration systems for zinc determination and evaluation with the proposed method using $\text{SiO}_2/\text{Al}_2\text{O}_3/\text{Nb}_2\text{O}_5$ as solid sorbent

Sorbent	Chelating agent/ Modifier	Eluent	PF	CI (mL)	SV (mL)	LD ($\mu\text{g L}^{-1}$)	Linear range ($\mu\text{g L}^{-1}$)	Detector	Ref.
Alizarin Red S	Alumina	HNO_3	144	0.17	25	0.2	1-100	FAAS	52
Silica gel	DPTH	Citric acid / tartaric acid	-	-	8.8	1.7	2-500	ICP OES	53
Amberlite XAD-7	Xylenol Orange	HCl	100	1	100	21	100-2000	FAAS	54
Amberlite XAD-2	oVTSC	HCl	140	7.14	1000	-	-	FAAS	55
XAD-7	8-BSQ	HCl	10	-	-	1.6	5-200 100-500	Spectrophotometry	56
Pumice stone	<i>Penicillium digitatum</i>	HCl	50	10	500	1.3	2.5-8	FAAS	57
Dowex 1X8-50	ARS	HNO_3	5	-	50-200	23	-	FAAS	58
Amberlite XAD-7	ARS	HNO_3	50	1	50	29	250-2000	FAAS	59
Silica gel	2-aminothiazole	HCl	-	-	50	97	-	FAAS	60
$\text{SiO}_2/\text{Al}_2\text{O}_3/\text{Nb}_2\text{O}_5$	pan	HNO_3	52.6	0.38	20	2.3	30 – 180	Spectrophotometry	This work

PF = preconcentration factor; CI = consumptive index; SV = sample volume; LOD = limit of detection; pan = (1-(2-pyridylazo)-2-naphtol); DPTH = 1,5-bis(di-2-pyridyl)methylene thiocarbonylhydrazide; ARS = Alizarin red S; oVTSC = vanillinthiosemicarbazone; 8-BSQ = 8-(benzenesulfonamido)quinoline; FAAS = flame atomic absorption spectrometry; ICP-OES = inductively coupled plasma optical emission spectrometry.

Table 2. Application of the proposed method for zinc determination in different types of water samples

Sample	Concentration of zinc added (mg L ⁻¹)	Concentration of zinc found* (mg L ⁻¹)	Recovery (%)
Mineral water	0	2.6 ± 0.4	-
	20.0	23.1 ± 0.3	102.2
Tap water	0	6.0 ± 0.4	-
	6.0	12.8 ± 1.0	106.7
Lake water	0	62.0 ± 1.9	-
	60.0	117.1 ± 1.4	96.0

* Results are expressed as mean values ± S.D. based on three replicate (n = 3) determinations. Confidence interval, 95%.

coupled to different spectroanalytical techniques (Table 1). As observed, the adsorbent preconcentration method presented here shows better or similar performance when compared with the works previously published in terms of limits of detection, sample consumption and sample throughput.⁵²⁻⁶⁰

Determination of Zn²⁺ in water samples and certified reference material

The method was applied to the direct determination of Zn²⁺ using external calibration in different types of water samples. Based on recovery studies with percentages varying from 96.0 to 106.7%, it is possible to conclude that the presence of foreign ions in these samples has no effect on the recovery of Zn²⁺ ions, thus attesting the accuracy of the method (Table 2). Moreover, the method was also successfully applied to Zn²⁺ determination in a certified reference material (TORT-2 Lobster Hepatopancreas) submitted to acid decomposition. The analytical results for this material (166.4 ± 4.6 mg kg⁻¹) are in good agreement with the certified values (180.0 ± 6.0 mg kg⁻¹), with 95% confidence level (*t*-student test), thereby also attesting its accuracy.

Conclusions

In this contribution, we reported for the first time the synthesis of a new material based on silica prepared by the sol-gel process and modified with an oxide mixture (Al₂O₃ and Nb₂O₅), as well as its characterization by SEM, EDS, surface area determination and infrared spectroscopy. The material exhibited outstanding features for use as a new solid adsorbent material, homogeneous dispersion of Al₂O₃ and Nb₂O₅ in the silica matrix, excellent swelling resistance and high adsorption capacity towards Zn²⁺ ions. Taking into account these features, a simple and sensitive flow injection spectrophotometric method for online preconcentration and determination of trace amounts of zinc was developed. The method presented feasibility for different types of samples (water and biological samples) with good precision and

accuracy. Finally, the results of this study demonstrate that the research on the development of new materials based on preparation of multiple oxides dispersed on silica matrix obtained by the sol-gel process deserves to be more exploited, aiming at improving the performance of the analytical protocol for solid phase extraction.

Acknowledgements

The authors thank CNPq (Conselho Nacional de Desenvolvimento Científico e Tecnológico), FAPEMIG (Fundação de Amparo à Pesquisa do Estado de Minas Gerais), CAPES (Coordenação de Aperfeiçoamento de Pessoal de Nível Superior), FAPERJ (Fundação Carlos Chagas Filho de Amparo à Pesquisa do Estado do Rio de Janeiro), IEN (Instituto de Engenharia Nuclear) and Instituto Nacional de Ciência e Tecnologia de Bioanalítica for the financial support and fellowships.

References

1. He, L.; Toh, C.; *Anal. Chim. Acta* **2006**, *556*, 1.
2. Gama, E.M.; Lima, A. S.; Lemos, V. A.; *J. Hazard. Mater.* **2006**, *136*, 757.
3. Amais, R. S.; Ribeiro, J. S.; Segatelli, M. G.; Yoshida, I. V. P.; Luccas, P. O.; Tarley, C. R. T.; *Sep. Purif. Technol.* **2007**, *58*, 122.
4. Rao, T. P.; Kala, R.; Daniel, S.; *Anal. Chim. Acta* **2006**, *578*, 105.
5. Tarley, C. R. T.; Barbosa, A. F.; Segatelli, M. G.; Figueiredo, E. C.; Luccas, P. O.; *J. Anal. At. Spectrom.* **2006**, *21*, 1305.
6. Etienne, M.; Walcarius, A.; *Talanta* **2003**, *59*, 1173.
7. Alfaya, A. A. S.; Gushikem, Y.; *J. Colloid Interface Sci.* **1999**, *209*, 428.
8. Marafon, E.; Kubota, L. T.; Gushikem, Y.; *J. Solid State Electrochem.* **2009**, *13*, 377.
9. Arguello, J.; Leidens, V. L.; Magosso, H. A.; Ramos, R. R.; Gushikem, Y.; *Electrochim. Acta* **2008**, *54*, 560.
10. Canevari, T. C.; Arguello, J. M.; Francisco, S. P.; Gushikem, Y.; *J. Electroanal. Chem.* **2007**, *609*, 61.

11. Ribeiro, E. S.; Dias, S. L. P.; Gushikem, Y.; Kubota, L. T.; *Electrochim. Acta*, **2004**, *49*, 829.
12. Ribeiro, E. S.; Dias, S. L. P.; Fujiwara, S. T.; Gushikem, Y.; Bruns, R. E.; *J. Applied Electrochem.* **2003**, *33*, 1069.
13. Ribeiro, E. S.; Gushikem, Y.; Biazotto, J. C.; Serra, A. O.; *J. Porphyrins Phthalocyanines* **2002**, *6*, 527.
14. Zaitseva, G.; Gushikem, Y.; Ribeiro, E. S.; Rosatto, S. S.; *Electrochim. Acta* **2002**, *4*, 1469.
15. Castellani, A. M.; Gushikem, Y.; *J. Colloid Interface Sci.* **2000**, *230*, 195.
16. Ribeiro, E. S.; Rosatto, S. S.; Gushikem, Y.; Kubota, L. T.; *J. Solid State Electrochem.* **2003**, *7*, 665.
17. Gao, X. T.; Fierro, J. L. G.; Wachs, I. E.; *Langmuir* **1999**, *15*, 3169.
18. Gonçalves, J. E.; Gushikem, Y.; Castro, S. C.; *J. Non-Cryst. Solids* **1999**, *260*, 125.
19. Menon, V.; Popa, V. T.; Contescu, C.; Schwarz, J. A.; *Rev. Roum. Chim.* **1998**, *43*, 393.
20. Miller, J. M.; Lakshmi, L. J.; *J. Phys. Chem. B* **1998**, *102*, 6465.
21. Kochkar, H.; Figueras, F.; *J. Catal.* **1997**, *171*, 420.
22. Dutoit, D. C. M.; Schneider, M.; Fabrizioli, P.; Baiker, A.; *J. Mater. Chem.* **1997**, *7*, 271.
23. Walcarius, A.; *Electroanalysis* **1998**, *10*, 1217.
24. Walcarius, A.; *Chem. Mater.* **2001**, *13*, 3351.
25. Walcarius, A.; *Electroanalysis* **2001**, *13*, 701.
26. Ferreira, C. U.; Gushikem, Y.; Kubota, L. T.; *J. Solid State Electrochem.* **2000**, *4*, 298.
27. Silveira, C. B.; Oliveira, A. F.; Campos, S. D.; Campos, E. A.; Carasek, E.; *Colloids Surf., A* **2005**, *259*, 15.
28. Budziak, D.; Silva, E. L. S.; Campos, S. D.; Carasek, E.; *Microchim. Acta* **2003**, *141*, 169.
29. Martendal, E.; Maltez, H. F.; Carasek, E. J.; *J. Hazard. Mater.* **2009**, *161*, 450.
30. Liu, Y.; Liang, P.; Guo, L.; *Talanta* **2005**, *68*, 25.
31. Nagata, N.; Kubota, L. T.; Bueno, M. I. M. S.; Zamora, P. G. P.; *J. Colloid Interface Sci.* **1998**, *200*, 121.
32. Macarvscha, G. T.; Bortoleto, G. G.; Cadore, S.; *Talanta* **2007**, *71*, 1150.
33. Fujiwara, S. T.; Pessoa, C. A.; Gushikem, Y.; *Anal. Lett.* **2002**, *35*, 1117.
34. Pavan, F. A.; Francisco, M. S. P.; Landers, Y. Gushikem; *J. Braz. Chem. Soc.* **2005**, *16*, 815.
35. Bayot, D. A.; Devillers, M. M. In *Progress in Solid State Chemistry Research*; Buckley, R. W., ed.; Nova Science Publishers: New York, 2007, ch. 3.
36. Miessler, G. L.; Tarr, D. A.; *Inorganic Chemistry*, 3rd ed., Pearson Prentice Hall: Upper Saddle River, 2004.
37. Garrett, R. H.; Grisham, C. M.; *Biochemistry*, 3rd ed., Thomson Brooks/Cole: Belmont, 2005.
38. Prasad, A. S.; *Brit. Med. J.* **2003**, *326*, 409.
39. Tarley, C. R. T.; Ferreira, S. L. C.; Arruda, M. A. Z.; *Microchem. J.* **2004**, *77*, 163.
40. Aronne, A.; Marenga, E.; Califano, V.; Fanelli, E.; Pernice, P.; Trifuoggi, M.; Vergara, A.; *J. Sol-Gel Sci. Technol.* **2007**, *43*, 193.
41. Cónsul, J. M. D.; Baibich, I. M.; Benvenuti, E. V.; Thiele, D.; *Quim. Nova* **2005**, *28*, 393.
42. Ziolk, M.; *Catal. Today* **2003**, *78*, 47.
43. Ahrland, S.; Herman, R. G.; *Anal. Chem.* **1975**, *4*, 2422.
44. Ralph, G. P.; *J. Am. Chem. Soc.* **1963**, *85*, 3533.
45. Bulut, V. N.; Gundogdu, A.; Duran, C.; Senturk, H. B.; Soylak, M.; Elci, L.; Tufekci, M.; *J. Hazard. Mater.* **2007**, *146*, 155.
46. Zhao, J. C.; Han, B.; Zhang, Y. F.; Wang, D. D.; *Anal. Chim. Acta* **2007**, *603*, 87.
47. Kumar, M.; Rathore, D. P. S.; Singh, A. K.; *Talanta* **2000**, *51*, 1187.
48. Sarkar, A. R.; Datta, P. K.; Sarkar, M.; *Talanta* **1996**, *43*, 1857.
49. Tewari, P. K.; Singh, A. K.; *Talanta* **2001**, *53*, 823.
50. Tarley, C. R. T.; Santos, W. N. L.; Santos, C. M.; Ferreira, S. L. C.; Arruda, M. A. Z.; *Anal. Lett.* **2004**, *37*, 1437.
51. Long, G. L.; Winefordner, J. D.; *Anal. Chem.* **1983**, *55*, 712.
52. Shabani, A. M. H.; Dadfarnia, S.; Moosavinejad, T.; *Quim. Nova* **2009**, *32*, 1202.
53. Zougagh, M.; Runder, P. C.; Torres, A. G.; Pavón J. M. C.; *J. Anal. At. Spectrom.* **2000**, *15*, 1589.
54. Pankaj, K. T.; Ajai, K. S.; *J. Anal. Chem.* **2000**, *367*, 562.
55. Jain, V. J.; Sait, S. S.; Shrivastav, P.; Agrawal, Y. K.; *Talanta* **1997**, *4*, 397.
56. Compañó, R.; Ferrer, R.; Guiteras, J.; Prat, M. D.; *Analyst* **1994**, *119*, 1225.
57. Bayatak, S.; Kendüzler, E.; Türker, A. R.; Gök, N.; *J. Hazard. Mater.* **2008**, *152*, 975.
58. Korn, M. G. A.; Santos Jr., A. F.; Jaeger, H. V.; Silva, N. M. S.; Costa, A. C. S.; *J. Braz. Chem. Soc.* **2004**, *15*, 212.
59. Santos Jr, A. F.; *Quim. Nova* **2002**, *25*, 1086.
60. Roldan, P. S.; Alcântara, I. L.; Rocha, J. C.; Padilha, C. C. F.; Padilha, P. M.; *Ecl. Quim.* **2004**, *29*, 33.

Received: September 21, 2009

Web Release Date: March 15, 2010

FAPESP helped in meeting the publication costs of this article.